https://ntrs.nasa.gov/search.jsp?R=19650019535 2018-07-23T00:29:51+00:00Z

Technical Report No. 32-728

Prediction of Heat Transfer from Laminar Boundary Layers, with Emphasis on Large Free-Stream Velocity Gradients and Highly Cooled Walls

L. H. Back
A. B. Witte

N65-29136
(ACCESSION NUMBER) (THRU)
23 1
(PAGES) (CODE)
CR 63904 33
(NASA CR OR TMX OR AD NUMBER) (CATEGORY)
FACILITY FORM 602

GPO PRICE $
CFSTI PRICE(S) $
Hard copy (HC) 1.00
Microfiche (MF) .50
ff 653 July 65

JET PROPULSION LABORATORY
CALIFORNIA INSTITUTE OF TECHNOLOGY
PASADENA, CALIFORNIA

June 1, 1965

Technical Report No. 32-728

Prediction of Heat Transfer from Laminar Boundary Layers, with Emphasis on Large Free-Stream Velocity Gradients and Highly Cooled Walls

L. H. Back

A. B. Witte

D. R. Bartz, Manager
Research and Advanced Concepts Section

JET PROPULSION LABORATORY
CALIFORNIA INSTITUTE OF TECHNOLOGY
PASADENA, CALIFORNIA

June 1, 1965

Copyright© 1965
Jet Propulsion Laboratory
California Institute of Technology

Prepared Under Contract No. NAS 7-100
National Aeronautics & Space Administration

CONTENTS

I. Introduction 1

II. Similarity Considerations 2

III. Variable $\rho\mu$ in Stagnation Point Heat Transfer 5

IV. Effect of Large Values of the Free-Stream Velocity Gradient Parameter $\bar{\beta}$ 7

V. Heat Transfer and Wall Friction Specification 12

VI. Application of Similarity Solutions 13

VII. Conclusions 15

Nomenclature 15

Appendixes 16

A. Solutions for $\bar{\beta} \to \infty$ 16

B. Calculation of $\bar{\beta}$ for Axisymmetric Nozzle Flow 17

References 17

TABLES

1. Comparison of approximate to exact stagnation point heat transfer predictions 6

2. Interpolation procedure results 10

A-1. Results as $\bar{\beta} \to \infty$ 16

FIGURES

1. Comparisons of approximate to exact stagnation point heat transfer predictions ($\beta = \bar{\beta} = 1/2$) for a monatomic gas ($Pr = 2/3$) with $\mu \propto T^{\omega}$ 5

2. Comparisons of approximate to exact stagnation region friction coefficient-Reynolds number predictions ($\beta = \bar{\beta} = 1/2$) for a monatomic gas ($Pr = 2/3$) with $\mu \propto T^{\omega}$ 6

FIGURES (Cont'd)

3. Interpolation of heat transfer parameter $(1/\sqrt{\bar{\beta}})g'_w/(1 - g_w)$ for $2 < \bar{\beta} < \infty$, $Pr = 1$, $C = 1$ 8

4. Variation of the heat transfer parameter $g'_w/(1 - g_w)$ with $\bar{\beta}$ and g_w for $Pr = 1$ and $C = 1$ 9

5. Interpolation of wall friction parameter $f''_w/\sqrt{\bar{\beta}}$ for $2 < \bar{\beta} < \infty$, $Pr = 1$, $C = 1$ 10

6. Variation of dimensionless velocity gradient at the wall, f''_w with $\bar{\beta}$ and g_w for $Pr = 1$ and $C = 1$ 11

7. Variation of free-stream velocity gradient parameter $\bar{\beta}$ with axial distance for two nozzles 14

ABSTRACT

29136

Laminar boundary layer heat transfer and shear stress predictions from existing similarity solutions are extended in an approximate way to perfect gas flows with a large free-stream velocity gradient parameter $\bar{\beta}$ and variable density–viscosity product $\rho\mu$ across the boundary layer resulting from a highly cooled wall. The dimensionless enthalpy gradient at the wall g'_w, to which the heat flux is related, is found not to vary appreciably with $\bar{\beta}$. Thus, the application of similarity solutions on a local basis to predict heat transfer from accelerated flows to an arbitrary surface may be a reasonable approximation involving a minimum amount of calculation time. Unlike g'_w, the dimensionless velocity gradient at the wall f''_w, to which the shear stress is related, is strongly dependent on $\bar{\beta}$.

I. INTRODUCTION

In reviewing the vast literature on laminar boundary layer heat transfer and shear stress predictions from similarity solutions for perfect gases, one finds an incomplete treatment of large free-stream velocity gradient effects when the walls are highly cooled. When the ratio of wall to total enthalpy, g_w, does not appreciably differ from unity, similarity solutions like those of Cohen and Reshotko (Ref. 1) for a perfect gas with constant density–viscosity product $\rho\mu$ across the boundary layer and an assumed Prandtl number of unity are available. Cohen and Reshotko's calculation, in which the Stewartson transformation was employed, covered free-stream velocity gradients up to that corresponding to infinite flow acceleration. Levy (Ref. 2) also obtained closely related similarity solutions for $\rho\mu$ constant across the boundary layer, g_w from 0.6 to 2, Prandtl numbers of 0.7 and 1.0, and a smaller range of free-stream velocity variations than investigated by Cohen and Reshotko. The inadequacy of Cohen and Reshotko's predictions, in which $\rho\mu$ was evaluated at the wall over the range of g_w from 0 to 2, has been pointed out by Probstein (Ref. 3) for highly cooled walls, i.e., $g_w \to 0$, by way of an application to stagnation point heat transfer. Probstein found the heat transfer rate for a realistic variation of $\rho\mu$ to be significantly lower than that calculated by using the wall value of $\rho\mu$. It should be pointed out that limitations apply as well to those solutions of the integral form of the boundary layer equations that depend on the similarity solutions in which the wall values of $\rho\mu$ were used, e.g., Cohen and Reshotko (Ref. 4) and Reshotko (Ref. 5). A better approximation of the heat transfer rate is from a method employed by Lees (Ref. 6) who took the group $C = \rho\mu/\rho_e\mu_e = 1$ across the boundary layer and set $\rho_w\mu_w = \rho_e\mu_e$ in the heat flux expression. Lees, who used the combined Levy-Mangler transformation, included predicted heat transfer rates for values of the free-stream velocity gradient parameter $\bar{\beta}$ from 0 to 2 and g_w from 0 to 1. Whereas for accelerated flows over blunt-nosed bodies this range of $\bar{\beta}$ is usually

adequate (e.g., at the stagnation point, $\bar{\beta} = 1/2$ and 1 for a body of revolution and circular cylinder, respectively) for internal flows, such as through supersonic nozzles, local values of $\bar{\beta}$ can be much larger as will be seen. For supersonic flows over flat-nosed bodies, local values of $\bar{\beta}$ may also exceed 2, e.g., see Kemp et al (Ref. 7).

In this paper Lees' approximate solution is extended to large values of $\bar{\beta}$ by the help of Coles' (Ref. 8) limiting solution as $\bar{\beta} \to \infty$. In so doing note is made of the interrelation of the similarity requirements if solutions are to be obtained over the entire speed range $0 \leq u_e^2/2H_{t_0} \leq 1.0$. Because the interrelation requires taking both the Prandtl number and C equal to unity, suitable corrections are made to allow application to perfect gases for which viscosity is not proportional to temperature and the Prandtl number is different from unity.

The extension of Lees' approximate method is accomplished by interpolations from existing solutions by Cohen and Reshotko from $\bar{\beta} = 2$ to Coles' limiting solutions as $\bar{\beta} \to \infty$. The interpolations are made in the representation of Coles' results, so that existing solutions are joined smoothly and both heat transfer and shear stress parameters are obtained. The heat transfer interpolations compare closely with those interpolations by Beckwith and Cohen (Ref. 9). Since Beckwith and Cohen's interpolations were made differently, they did not obtain the shear stress parameter for large values of $\bar{\beta}$. Finally, the utilization of the similarity solutions in predicting heat transfer to arbitrary surfaces is discussed.

The analysis is for perfect gases at high temperatures, but not exceeding those temperatures at which dissociation, ionization or radiation effects become important.

II. SIMILARITY CONSIDERATIONS

For axisymmetric flow of a perfect gas the laminar boundary layer equations, in which both the velocity and thermal layer thicknesses are assumed small compared to either the body radius r for an external flow or the channel radius for an internal flow, are the continuity equation:

$$\frac{\partial}{\partial x}(\rho u r^j) + r^j \frac{\partial}{\partial y}(\rho v) = 0 \tag{1}$$

with $j = 1$ for axisymmetric flow; the momentum equation:

$$\rho u \frac{\partial u}{\partial x} + \rho v \frac{\partial u}{\partial y} = -\frac{dp}{dx} + \frac{\partial}{\partial y}\left(\mu \frac{\partial u}{\partial y}\right) \tag{2}$$

and the energy equation:

$$\rho u \frac{\partial H_t}{\partial x} + \rho v \frac{\partial H_t}{\partial y} = \frac{\partial}{\partial y}\left[\frac{\mu}{Pr}\frac{\partial H_t}{\partial y} + \mu\left(1 - \frac{1}{Pr}\right)\frac{\partial}{\partial y}\left(\frac{u^2}{2}\right)\right] \tag{3}$$

The analysis is applicable to flow over a plane surface if $j = 0$. As was done by Lees, the boundary layer equations are transformed from the x, y coordinate system by the combined Levy-Mangler transformation:

$$\eta = \frac{r^j u_e}{(2\xi)^{1/2}} \int_0^y \rho \, dy \quad ; \quad \xi = \int_0^x \rho_e \mu_e u_e r^{2j} \, dx \tag{4}$$

Assuming that the velocity and total enthalpy profiles are similar in terms of η, i.e., $u/u_e = f'(\eta)$, $H_t/H_{to} = g(\eta)$, and that $H_{te} = H_{to} = constant$, the transformed momentum and energy equations are:

$$(Cf'')' + ff'' + \beta\left[\frac{\rho_e}{\rho} - (f')^2\right] = 0 \tag{5}$$

$$\left(\frac{C}{Pr}g'\right)' + fg' + \frac{u_e^2}{2H_{to}}\left[2C\left(1 - \frac{1}{Pr}\right)f'f''\right]' = 0 \tag{6}$$

where $C = \rho\mu/\rho_e\mu_e$ and $\beta = (2\xi/u_e)(du_e/d\xi)$. The primes denote differentiation with respect to η. The surface is assumed impervious to flow and at a specified temperature so that the enthalpy at the wall is known. The boundary conditions are thus:

$$\begin{aligned} &f(0) = f'(0) = 0 \qquad g(0) = g_w \qquad \text{at } \eta = 0 \\ &f'(\eta) \to 1 \qquad g(\eta) \to 1 \qquad \text{as } \eta \to \infty \end{aligned} \tag{7}$$

The heat flux to the wall is

$$q = k_w\left(\frac{\partial T}{\partial y}\right)_w = \frac{\mu_w}{Pr}H_{to}\left(\frac{\partial \eta}{\partial y}\right)_w\left(\frac{dg}{d\eta}\right)_w = \frac{(H_{to} - H_w)(\rho_e u_e)}{Pr}\left[\frac{r^j\mu_e}{(2\xi)^{1/2}}\right]\left(\frac{\rho_w\mu_w}{\rho_e\mu_e}\right)\left(\frac{g'_w}{1 - g_w}\right) \tag{8}$$

The wall shear stress is

$$\tau = \mu_w\left(\frac{\partial u}{\partial y}\right)_w = \mu_w u_e\left(\frac{\partial \eta}{\partial y}\right)_w\left(\frac{df''}{d\eta}\right)_w = \mu_e u_e^2\left[\frac{r^j\mu_e}{(2\xi)^{1/2}}\right]\left(\frac{\rho_w\mu_w}{\rho_e\mu_e}\right)f''_w \tag{9}$$

Similarity solutions are possible if the following requirements are satisfied:

(a) $g_w = constant$

(b) either $Pr = Pr(\eta)$, or a *constant* and

$$\begin{aligned} &\frac{u_e^2}{2H_{to}} \to 0, \qquad \text{low speed flow limit} \\ &\frac{u_e^2}{2H_{to}} \to 1, \qquad \text{high speed flow limit} \end{aligned} \tag{10}$$

or $Pr = 1$

(c) $C = C(\eta)$, or a *constant*

(d) $\beta\left[\frac{\rho_e}{\rho} - (f')^2\right]$ is independent of ξ

By assuming that these requirements are satisfied, the solution of the coupled Eq (5) and (6) depends on g_w, Pr, $u_e^2/2H_{to}$, C, and β. Some of these terms, however, are interrelated. To illustrate these relationships, a consequence of requirement Eq. (10d) is that $\beta = constant$, from which the free-stream velocity distribution must be of the form $u_e = b\xi^{\beta/2}$ with $b = constant$. The ratio of kinetic to total energy then is dependent on ξ,

$$\frac{u_e^2}{2H_{to}} = \frac{b^2\xi^\beta}{2H_{to}}$$

Thus, if $Pr \neq 1$, similar solutions are only possible for either of the limiting cases of low and high speed flow as can be seen in the energy Eq. (6); for intermediate values, similarity solutions are not possible since $u_e^2/2H_{to}$ depends on ξ (the obvious exception would be a constant free-stream velocity flow, $\beta = 0$). However, it appears that by assuming $Pr = 1$, similarity solutions are possible over the entire flow speed range $0 \leq u_e^2/2H_{to} \leq 1$, since the term in which $u_e^2/2H_{to}$ appears in Eq. (6) vanishes. Though this seems correct, further restrictions are imposed by the requirement that $C = C(\eta)$. This can be seen by writing

$$C = \frac{\rho\mu}{\rho_e\mu_e} = \frac{T_e}{T}\frac{\mu}{\mu_e} = \left(\frac{T_e}{T}\right)^{1-\omega} = \left(\frac{T_e/T_{to}}{T/T_{to}}\right)^{1-\omega}$$

In order to obtain an explicit relation, a perfect gas with a constant specific heat and $\mu\alpha T^\omega$ is considered, although these restrictions would not change the conclusions that follow. By using the relations

$$\frac{H}{H_{to}} = \frac{T}{T_{to}} = g - (f')^2\left(\frac{u_e^2}{2H_{to}}\right)$$

and that $g = f' = 1$ in the free-stream

$$C = \left[\frac{1 - \dfrac{u_e^2}{2H_{to}}}{g - (f')^2\dfrac{u_e^2}{2H_{to}}}\right]^{1-\omega} \tag{11}$$

By observation C is independent of ξ only if either $\omega = 1$, i.e., $\mu\alpha T$ or at the low speed flow limit. It thus appears that to obtain similarity solutions over the entire flow speed range one must take $Pr = C = 1$. About all that can be done then is to make corrections that allow application of the solutions to gases with ω and Pr not equal to unity.

Flows in the physical plane that correspond to $\beta = constant$ are determined from

$$\beta = \frac{2\xi}{u_e}\frac{du_e}{d\xi} = \frac{2\xi}{\dfrac{d\xi}{dx}}\frac{1}{u_e}\frac{du_e}{dx}$$

$$= 2\frac{\displaystyle\int_0 \rho_e\mu_e u_e r^{2j}\,dx}{\rho_e\mu_e u_e r^{2j}}\frac{1}{u_e}\frac{du_e}{dx} \tag{12}$$

The variation of the free-stream velocity along the surface is seen to be dependent on r and $\rho_e\mu_e$ in a complicated way. Even for a perfect gas with assumed $\mu\alpha T$, for which the variation of $\rho_e\mu_e$ along the surface can be expressed in terms of the static pressure and thus the free-stream velocity, u_e still depends on r. Although a general solution is not possible, two special cases are considered to indicate the range of β that need be investigated: 1) Levy (Ref. 2), for plane flow $j = 0$, assumed $\rho_e\mu_e = constant$ along the surface for which substituting the velocity distribution $u_e = bx^m$ in Eq. (12) gives $\beta = 2m/(m + 1)$; 2) for low speed internal, axisymmetric, one-dimensional flow for which the mass flow rate is $\rho_e u_e(\pi r^2)$ the relationship is $\beta = 2m$. To investigate the entire flow acceleration range from $m = 0$ to ∞ in the first case, the corresponding range of β from 0 to 2 only needs to be investigated. As Levy has pointed out, these correspond to the wedge flows treated by Hartree (Ref. 10). However for the second case, similarity solutions are needed for a larger β range.

III. VARIABLE $\rho\mu$ IN STAGNATION POINT HEAT TRANSFER

Before investigating the effect of large β the effect of variable C needs to be considered. To indicate its variation for a highly cooled wall, e.g., $g_w = 0.01$, the low-speed value of C at the wall from Eq. (11) is $C_w = (100)^{1-\omega}$; thus for $\omega = 0.75$, C increases from its free-stream value of 1 to 3.2 at the wall.

The effect of C varying across the boundary layer can be investigated by using Bade's (Ref. 11) solutions for a body of revolution ($\beta = \frac{1}{2}$) and a monatomic gas with $Pr = \frac{2}{3}$, $p = \rho RT$, $H = c_pT$, and viscosity–temperature relation $\mu\alpha T^\omega$ over a range of $0.5 \leq \omega \leq 1.0$ and $0.01 \leq g_w \leq 0.8$. It is useful to compare these exact solutions, in the sense that the variation of C across the boundary layer was taken into account, to approximate ones in which C is assumed invariable across the boundary layer and is evaluated at a reference temperature, i.e., $C = C_{ref} = T_e/\mu_e(\mu/T)_{ref}$. The results in Fig. 1

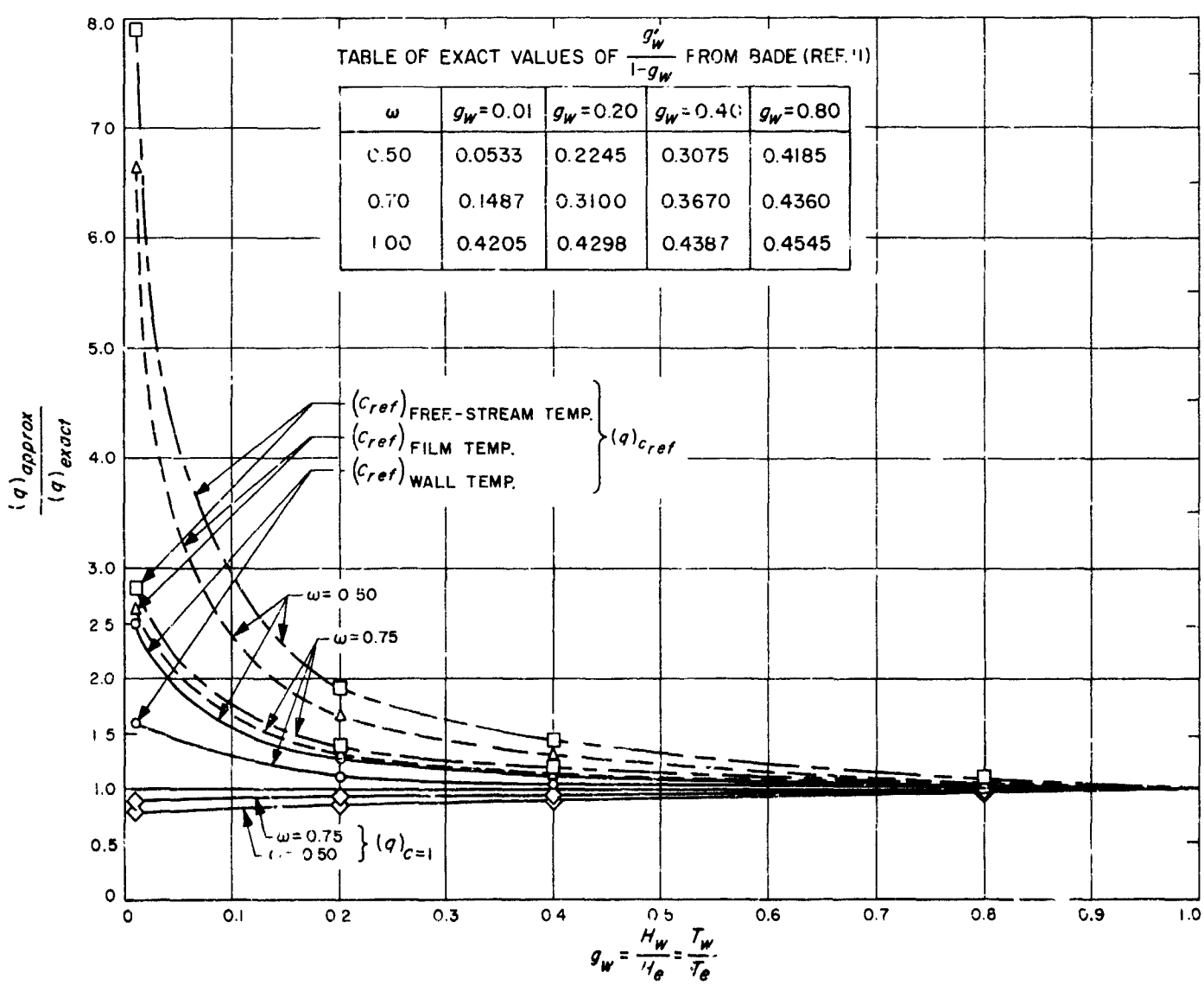

Fig. 1. Comparisons of approximate to exact stagnation point heat transfer predictions ($\beta = \bar{\beta} = \frac{1}{2}$) for a monatomic gas ($Pr = \frac{2}{3}$) with $\mu\alpha T^\omega$

The points were determined from the exact values of Bade (Ref. 11) and the curves were faired through the points. All the ratios are equal to unity for $\omega = 1.0$.

clearly show the limitation of these approximate solutions for highly cooled walls. Note in particular, the higher predictions with C_{ref}, i.e., $\rho\mu$ evaluated at the wall temperature.

Although the C_{ref} method fails, another method in which $g'_w/(1 - g_w)$ is determined from a solution with $C = 1$ and $\rho_w\mu_w$ is taken equal to $\rho_e\mu_e$ in the heat flux expression Eq. (8) does provide good agreement with the exact values as seen in Fig. 1 by the near-unity ratios. This method was employed by Lees (Ref. 6) as an approximation to the actual case. This approximate method, however, would not be expected to apply if the arbitrary choice of $\rho_e\mu_e$ in ξ, Eq. (4), and in C were evaluated at a reference condition different from the free-stream one. For a discussion of this point see Fay and Riddell (Ref. 12). The near-unity ratios also indicate the weak dependence of the predicted heat transfer coefficient $h = q/(H_e - H_w)$ from Eq. (8) with $H_{t_e} = H_e$ on the wall to free-stream temperature ratio, as shown by the small variation of the group $g'_w/(1 - g_w)_{C=1}$ tabulated in Fig. 1, i.e., for $\omega = 1.0$.

With a small correction factor which is essentially independent of ω the predictions for $C = 1$ can be adjusted to better agree with the exact values

$$q_{exact} \cong \left(\frac{\rho_w\mu_w}{\rho_e\mu_e}\right)^{0.1} (q)_{C=1} \tag{13}$$

Table 1. Comparison of approximate to exact stagnation point heat transfer predictions

Table values are the ratio: $\dfrac{(q)_{C=1}\left(\dfrac{\rho_w\mu_w}{\rho_e\mu_e}\right)^{0.1}}{(q)_{exact}}$

ω	$g_w = 0.01$	$g_w = 0.20$	$g_w = 0.40$	$g_w = 0.80$
0.5	0.994	0.928	0.943	0.982
0.75	1.004	0.954	0.971	0.991
1.00	1.0	1.0	1.0	1.0

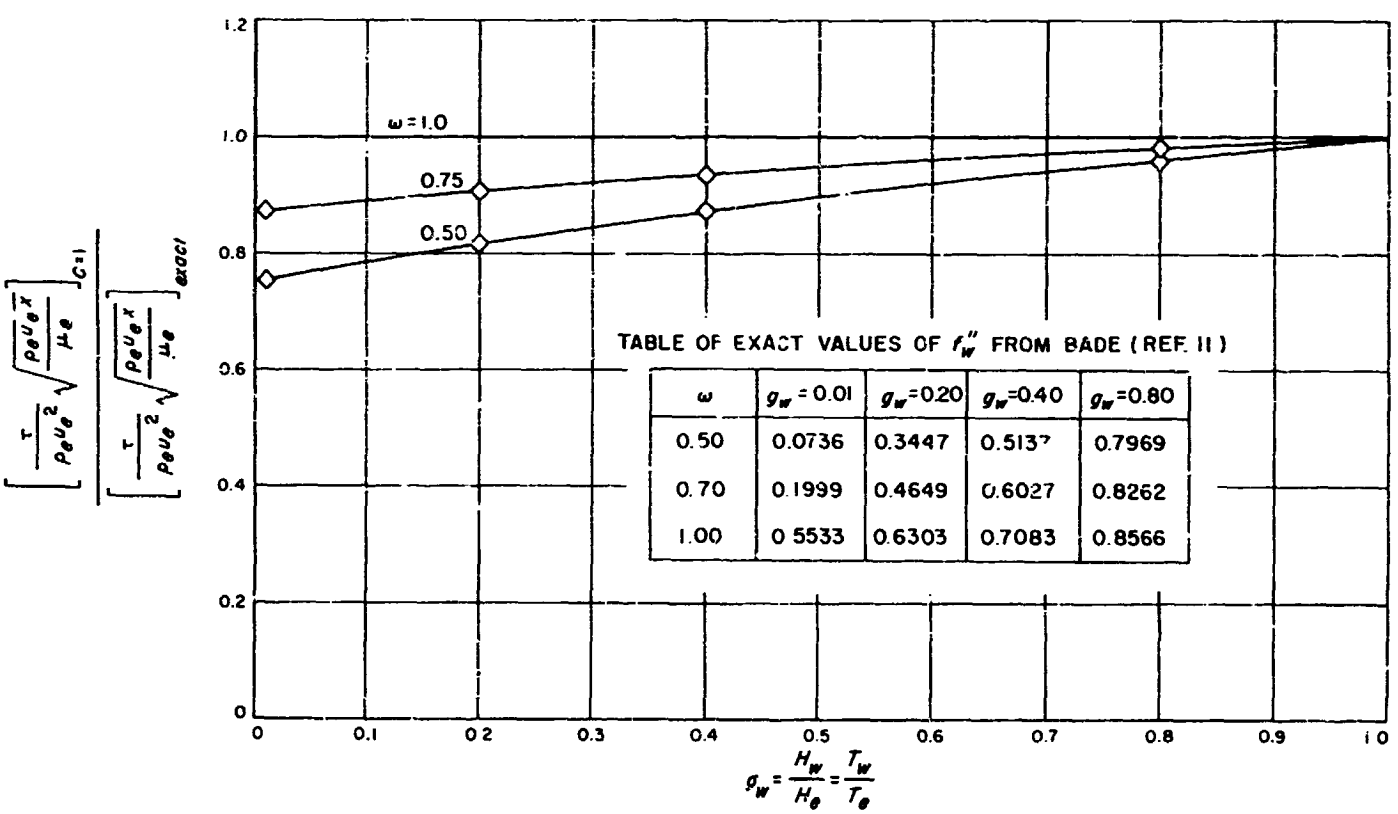

ω	$g_w = 0.01$	$g_w = 0.20$	$g_w = 0.40$	$g_w = 0.80$
0.50	0.0736	0.3447	0.5137	0.7969
0.70	0.1999	0.4649	0.6027	0.8262
1.00	0.5533	0.6303	0.7083	0.8566

Fig. 2. Comparisons of approximate to exact stagnation region friction coefficient-Reynolds number predictions ($\beta = \bar{\beta} = 1/2$) for a monatomic gas ($Pr = 2/3$) with $\mu \alpha T^{\omega}$

The points were determined from the exact values of Bade (Ref. 11) and the curves were faired through the points. The distance x is measured from the stagnation point.

Table 1 shows the correspondence to be within 1% at $g_w = 0.01$. The same factor is also indicated by the Fay and Riddell (Ref. 12) predictions in which the Sutherland viscosity law was used.

Shown in Fig. 2 to be as nearly a good approximation as for the heat flux is the friction coefficient–Reynolds number group. Predictions with C_{ref} are not shown since they exceed the exact values, similar to the heat flux. Whereas the heat transfer coefficient is insensitive to wall cooling, the group $(\tau/\rho_e u_e^2)\sqrt{\rho_e u_e x/\mu_e}$ diminishes with wall cooling. The accuracy of the following approximation is similar to that for the heat flux shown in Table 1.

$$\left[\frac{\tau}{\rho_e u_e^2}\sqrt{\frac{\rho_e u_e x}{\mu_e}}\right]_{exact} \cong \left(\frac{\rho_w \mu_w}{\rho_e \mu_e}\right)^{0.42}\left[\frac{\tau}{\rho_e u_e^2}\sqrt{\frac{\rho_e u_e x}{\mu_e}}\right]_{ref} \tag{14}$$

IV. EFFECT OF LARGE VALUES OF THE FREE-STREAM VELOCITY GRADIENT PARAMETER $\bar{\beta}$

To investigate the effect of large values of $\bar{\beta}$ over the entire flow speed range, previous considerations require taking C and Pr equal to unity. From the preceding section a correction for the actual variation of C across the boundary layer for low speed flow can be made with Eq. (13) and (14). Strictly speaking, for higher speed flows, from Eq. (11), taking $C = 1$ implies that $\mu \alpha T$; however, the correction of Eq. (13) and (14) may still be a fair approximation for actual gases where μ is not proportional to T, as can be seen in Eq. (11) where C would vary less across the boundary layer as $u_e^2/2H_{t_0}$ increases. The assumption that $Pr = 1$ should not impose a serious limitation since a correction for the actual Prandtl number can be made, and this is discussed in the following section. If the specific heat is assumed constant, then since the total enthalpy in the free stream is constant, the group involving the free-stream velocity gradient in Eq. (5) can be written as

$$\beta\left[\frac{\rho_e}{\rho} - (f')^2\right] = \bar{\beta}\left[g - (f')^2\right] \tag{15}$$

where

$$\bar{\beta} = \beta\frac{T_{t_0}}{T_e} = \frac{2\xi}{M_e}\frac{dM_e}{d\xi}$$

With these assumptions, Eq. (5) and (6) become

$$f''' + ff'' + \bar{\beta}\left[g - (f')^2\right] = 0 \tag{16}$$

$$g'' + fg' = 0 \tag{17}$$

These equations and boundary conditions Eq. (7) with g_w = *constant* are in the same form as those solved by Cohen and Reshotko (Ref. 1) for $\bar{\beta}$ to 2 and by Coles (Ref. 8) for $\bar{\beta} \to \infty$. However, in both of these analyses the Stewartson transformation was used, so that $\bar{\beta}$ and their independent variables, like η and ξ, are defined differently in terms of the flow variables. Cohen and Reshotko's solutions were obtained by a method of successive approximations, while Coles used a singular expansion procedure in which an inner (near the wall), and an outer series expansion was required to obtain a uniformly valid solution throughout the boundary layer. The results of the analysis by Coles, in which an approximate solution of two differential equations (Ref. 8, Eq. 92 and 93) has been improved by an exact solution as described in Appendix A, is shown by the straight lines in Fig. 3 in a representation identical to that of Fig. 6 in his paper. Cohen and Reshotko's values are shown by the points through which lines have been drawn.

Rather than solve Eq. (16) and (17) for $2 < \bar{\beta} < \infty$, a task more difficult to do numerically for large values of $\bar{\beta}$, an approximation of $g_w'/(1 - g_w)$, adequate for calculation purposes, may be obtained by interpolating between the values of Cohen and Reshotko and those of Coles shown in Fig. 3 with a third-order polynomial which matches the slope and value of the function at the end points; the dashed curves indicate the interpolations. The error in the interpolation is difficult to determine, but due to the way the solutions are smoothly joined when plotted in terms of $1/\sqrt{\bar{\beta}}$ in Fig. 3, it is expected to be small; in particular, Beckwith and Cohen's (Ref. 9)

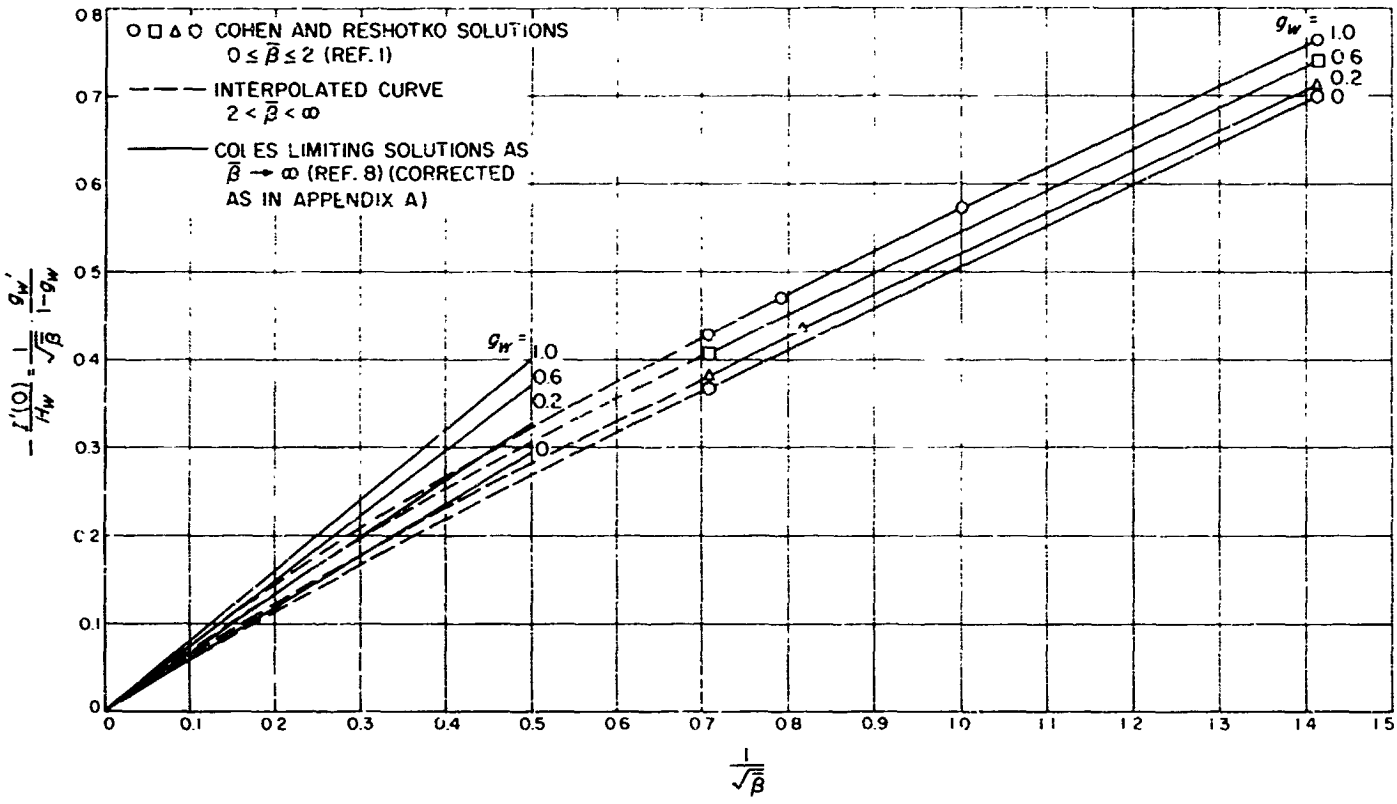

Fig. 3. Interpolation of heat transfer parameter $(1/\sqrt{\bar{\beta}})g'_w/(1 - g_w)$ for $2 < \bar{\beta} < \infty$, $Pr = 1$, $C = 1$

solutions of Eq. (16) and (17) for values of $\bar{\beta}$ to 4.4 are within 0.5% of the interpolated values. Values of $g'_w/(1 - g_w)$ so obtained are shown in Fig. 4, together with Coles' limiting values and the values of Cohen and Reshotko. Of note in Fig. 4 is that as $\bar{\beta} \to \infty$, $g'_w/(1 - g_w)$ remains finite; however, like Coles' analysis where the wall heat flux vanishes as $1/\sqrt{\bar{\beta}}$, it can be shown that the heat flux in Eq. (8) also approaches zero as $\bar{\beta} \to \infty$. In addition, Table 2 includes a few numerical values of $g'_w/(1 - g_w)$ obtained from the interpolation procedure shown in Fig. 3. Beckwith and Cohen's interpolated values of $g'_w/(1 - g_w)$ for $g_w = 0$ and 1.0 and about $\bar{\beta} > 4$ are within about 1% of the values shown in Table 2.

From Fig. 4, the effect of infinite flow acceleration is seen to increase $g'_w/(1 - g_w)$ by 25% above the zero free-stream velocity gradient value for a highly cooled wall, $g_w \cong 0$; for smaller amounts of wall cooling, the effect is larger.

Cohen and Reshotko (Ref. 1) have also obtained solutions to Eq. (16) and (17) for flow deceleration, $\bar{\beta} < 0$; their values of $g'_w/(1 - g_w)$ are shown in the inset in Fig. 4. Compared to the accelerated flow values the decelerated flow ones are strongly dependent on $\bar{\beta}$, especially near the predicted separation point (note the different $\bar{\beta}$ scales). The predictions are also double-valued near separation, the physical significance of which is discussed in Ref. 1. In addition, for decelerated flows over highly cooled walls, the effect of variable C has not been studied so that the correction in Eq. (13) for an accelerated flow may not apply. In view of these observations, one must be careful in applying the predictions to decelerated flows.

The effect of large free-stream velocity gradient on wall shear stress is obtained in an approximate way analogous to the heat flux. Values of f''_w for $2 < \bar{\beta} < \infty$ were obtained by interpolating between the results of Coles (Ref. 8) (corrected as in Appendix A) and Cohen and Reshotko (Ref. 1) with a third-order polynomial in powers of $1/\sqrt{\bar{\beta}}$, as shown by the dashed curves in Fig. 5. In particular the interpolations are within 0.1% of solutions to Eq. (16) and (17) by John Klineberg for values of $\bar{\beta}$ to 500 and $g_w = 1.0$.* The values of f''_w are shown for $0 \leq \bar{\beta} \leq 100$ in Fig. 6. Unlike $g'_w/(1 - g_w)$

*Private communication, John Klineberg, California Institute of Technology.

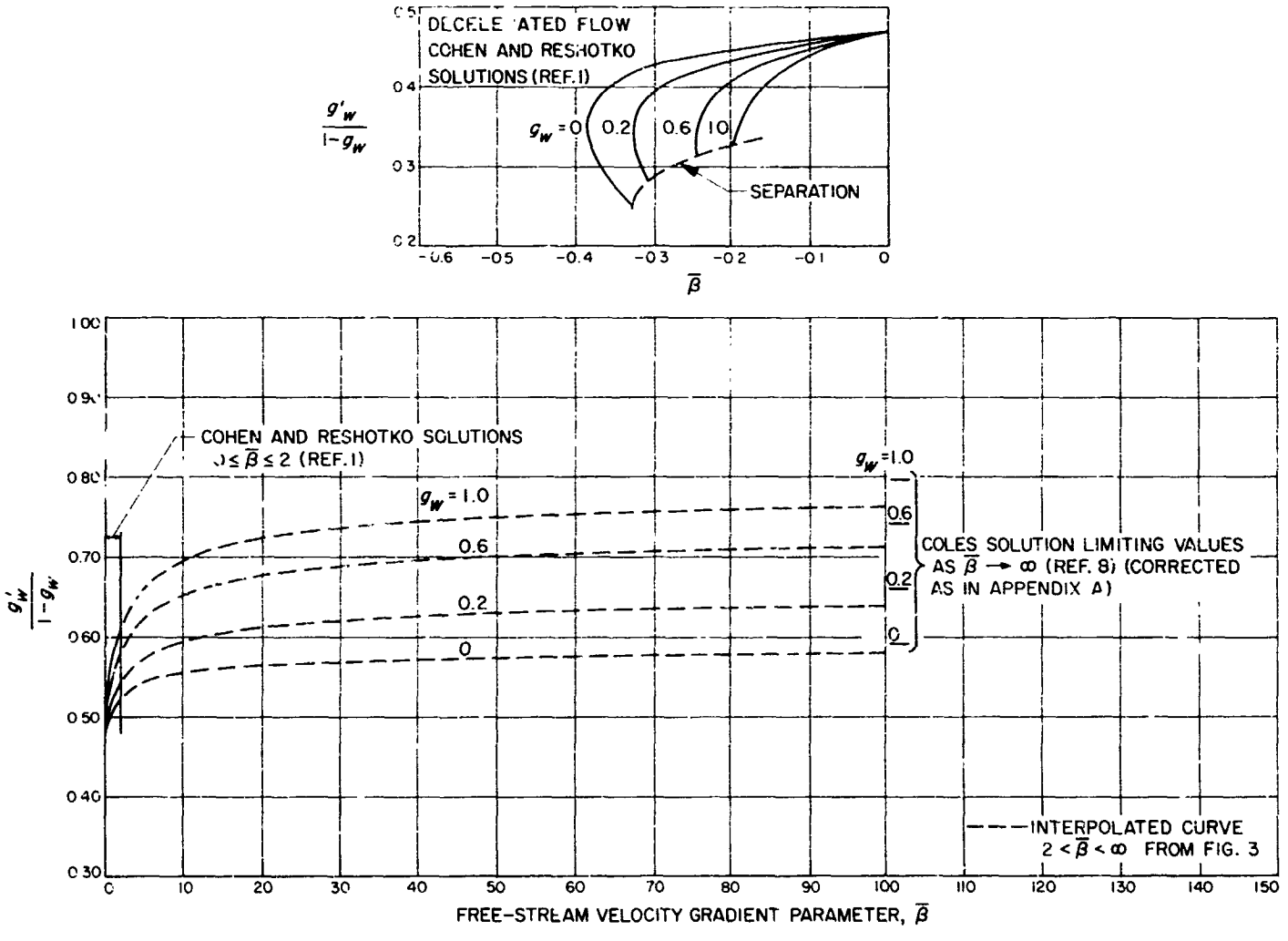

Fig. 4. Variation of the heat transfer parameter $g'_w/(1 - g_w)$ with $\bar{\beta}$ and g_w for $Pr = 1$ and $C = 1$

Table 2. Interpolation procedure results

$\bar{\beta}$	$\frac{g'_w}{1-g_w}$	f''_w	$\frac{g'_w}{1-g_w}$	f''_w	$\frac{g'_w}{1-g_w}$	f''_w	$\frac{g'_w}{1-g_w}$	f''_w
	$g_w = 0$		$g_w = 0.2$		$g_w = 0.6$		$g_w = 1.0$	
0[a]	0.4696	0.4696	0.4696	0.4696	0.4696	0.4696	0.4696	0.4696
0.5[a]	0.4948	0.5806	0.5038	0.6547	0.5225	0.7947	0.5395	0.9277
1.0[a]	—	—	—	—	—	—	0.5715	1.2326
1.5[a]	—	—	0.5326	0.8689	—	—	—	—
2[a]	0.5203	0.7381	0.5414	0.9480	0.5760	1.3329	0.6064	1.6870
3	0.530	—	0.556	1.076	0.598	1.577	0.631	2.042
4	0.537	—	0.565	1.188	0.612	1.784	0.647	2.346
5	0.542	—	0.572	1.273	0.623	1.967	0.660	2.614
9	0.553	—	0.590	1.557	0.649	2.564	0.689	3.486
16	0.561	—	0.603	1.918	0.669	3.348	0.713	4.635
25	0.567	—	0.615	2.274	0.683	4.133	0.729	5.786
36	0.570	—	0.622	2.632	0.692	4.919	0.740	6.937
49	0.573	—	0.627	2.976	0.699	5.706	0.748	8.089
64	0.575	—	0.631	3.325	0.703	6.492	0.753	9.244
100	0.578	—	0.636	4.021	0.711	8.065	0.762	11.55
∞[b]	0.5901	—	0.6590	∞	0.7408	∞	0.7979	∞

[a]Cohen and Reshotko's values (Ref. 1).

[b]Coles' values (Ref. 8) corrected as in Appendix A.

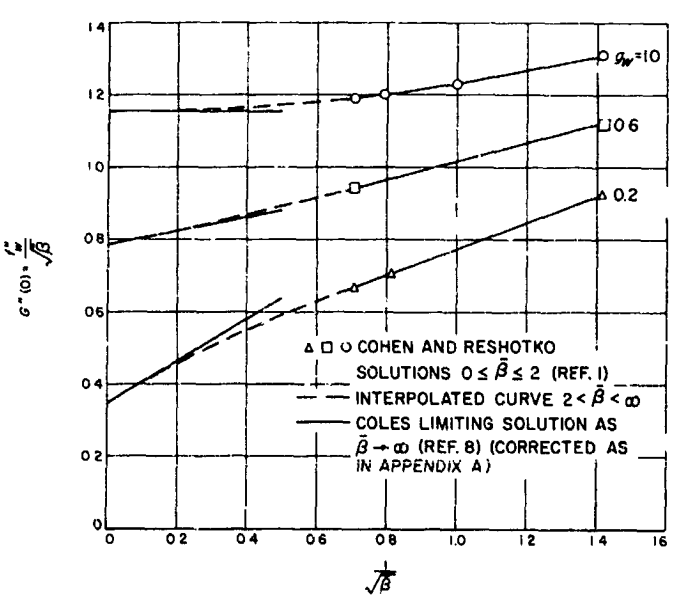

Fig. 5. Interpolation of wall friction parameter $f''_w/\sqrt{\bar{\beta}}$ for $2 < \bar{\beta} < \infty$, $Pr = 1$, $C = 1$

which remains finite, $f''_w \to \infty$ as $\bar{\beta} \to \infty$. This result follows directly from Coles' solution as shown in Fig. 5 where $f''_w/\sqrt{\bar{\beta}}$ remains finite as $1/\sqrt{\bar{\beta}} \to 0$, i.e., as $\bar{\beta} \to \infty$. However, although $f''_w \to \infty$ as $\bar{\beta} \to \infty$, it can be shown from Coles' analysis that the wall shear stress is finite. Of note in Figs. 5 and 6 is that values are shown for $g_w = 0.2$, 0.6, and 1.0. Coles did not include values for $g_w = 0$ since as $\bar{\beta} \to \infty$, $f''_w/\sqrt{\bar{\beta}} \to 0$, but the slope $d(f''_w/\sqrt{\bar{\beta}})/d(1/\sqrt{\bar{\beta}}) \to \infty$. An attempt was made to obtain f''_w for a small value of $g_w = 0.01$; however, it led to an unrealistic polynomial approximation as a result of the large slope of Coles' prediction relative to that of Cohen and Reshotko for a small value of g_w.

From Fig. 6 the values of f''_w are seen to be strongly dependent on $\bar{\beta}$. Even for $g_w = 0.20$, where the variation of f''_w with $\bar{\beta}$ is least, there is about a five-fold increase in f''_w at $\bar{\beta} = 20$ above the zero free-stream velocity gradient value.

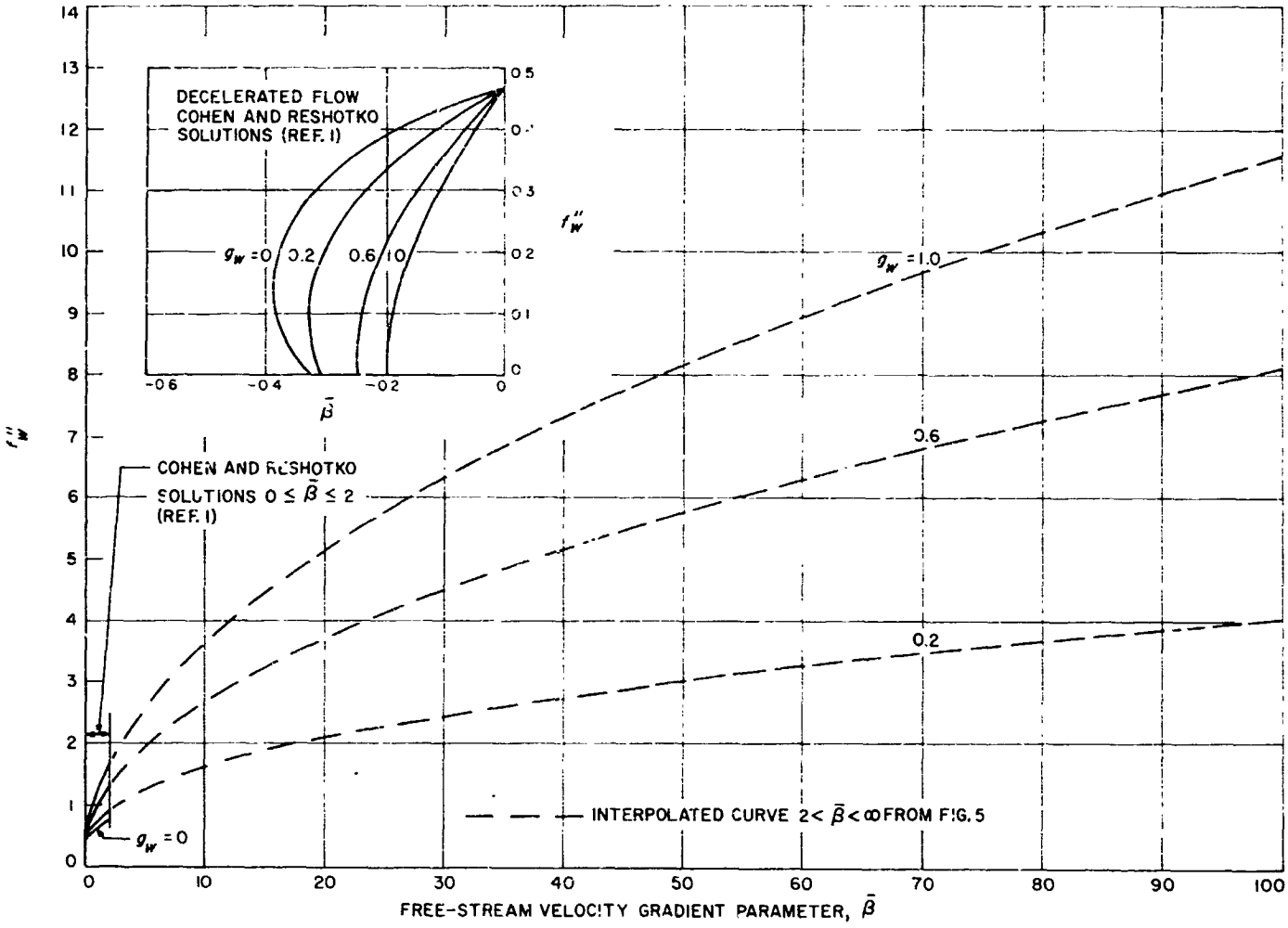

Fig. 6. Variation of dimensionless velocity gradient at the wall, f''_w, with $\bar{\beta}$ and g_w for $Pr = 1$ and $C = 1$

Values of f''_w for decelerated flow to separation from Cohen and Reshotko (Ref. 1) are included in the inset in Fig. 6.

The remarks made previously with regard to the calculation of the heat transfer apply as well to the wall shear stress for $\bar{\beta} < 0$.

V. HEAT TRANSFER AND WALL FRICTION SPECIFICATION

Having treated separately the effects of variable C and $\bar{\beta}$, the combined results from Eq. (8) (with $Pr = 1$ and $\rho_w\mu_w = \rho_e\mu_e$) and the correction of Eq. (13), the approximation of the heat flux to the wall is

$$q = (H_{aw} - H_w)(\rho_e u_e)\left[\frac{r^j \mu_e}{(2\xi)^{1/2}}\right]\left(\frac{\rho_w\mu_w}{\rho_e\mu_e}\right)^{0.1} Pr^{-2/3}\left(\frac{g'_w}{1 - g_w}\right) \tag{18}$$

This relation can be cast in a familiar form by introducing a length $\bar{x}$ defined by

$$\bar{x} = \frac{\xi}{\rho_e\mu_e u_e r^{2j}} = \frac{\int_0^x \rho_e\mu_e u_e r^{2j}\, dx}{\rho_e\mu_e u_e r^{2j}} \tag{19}$$

Then the Stanton number becomes

$$St = \frac{q}{(H_{aw} - H_w)\rho_e u_e} = \frac{1}{\sqrt{2}}\left(\frac{g'_w}{1 - g_w}\right)\left(\frac{\rho_w\mu_w}{\rho_e\mu_e}\right)^{0.1}\left(\frac{\rho_e u_e \bar{x}}{\mu_e}\right)^{-1/2} Pr^{-2/3} \tag{20}$$

The group $g'_w/(1 - g_w)$ is determined from Fig. 4 for values of $\bar{\beta}$ and g_w. The prediction in either Eq. (18) or (20) was corrected for a Prandtl number other than unity by multiplying by the factor $Pr^{-2/3}$, indicated by the low speed flat plate flow solution of Pohlhausen (Ref. 10) (other factors have been found, e.g., Fay and Riddell (Ref. 12) give $Pr^{-0.6}$). Even for the high speed flow limit this correction is in good agreement with the similarity predictions of Gross and Dewey (Ref. 13) for variable $\rho\mu$ and values of $\bar{\beta}$ from 0 to 1.0, when the wall is highly cooled. The separate Prandtl number correction is also supported by the similarity predictions of Kemp et al. (Ref. 7) for variable $\rho\mu$ and values of β from 0 to 2.0 which indicate that at a given Prandtl number (0.71 in their analysis) for highly cooled walls, the group $g'_w/(1 - g_w)$ was only slightly affected by values of $u_e^2/2H_{to}$ ranging to ¾, and mainly affected by β.

To be consistent with the Prandtl number correction the enthalpy difference $(H_{to} - H_w)$ has been replaced by the difference between the adiabatic wall and wall enthalpies $(H_{aw} - H_w)$. For highly cooled walls, where the wall temperature is much lower than the adiabatic wall temperature, the difference between these driving potentials is small. The adiabatic wall enthalpy can be calculated from

$$R = \frac{H_{aw} - H_e}{H_{to} - H_e} = Pr^{1/2} \tag{21}$$

Kemp et al (Ref. 7) found this recovery factor R dependence on Prandtl number to be valid for high speed flows with $\rho\mu$ variable for values of $\beta = 0$ and ½.

Although these latter considerations have been directed towards highly cooled walls, either of the relations Eq. (18) or (20) should provide a good approximation for wall cooling over the range of g_w from 0 to that corresponding to the adiabatic wall condition.

$$g_{rw} = \frac{H_{rw}}{H_{to}} = 1 - (1 - R)\frac{u_e^2}{2H_{to}} \tag{22}$$

The inclusion of values of $g'_w/(1 - g_w)$ in Fig. 4 for $g_w = 1$ thus allows interpolation for intermediate values of g_w less than g_{rw}.

By combining the results from Eq (9) with $\rho_w\mu_w = \rho_e\mu_e$ and the correction of Eq. (14), the approximation of the friction coefficient is

$$\frac{c_f}{2} = \frac{\tau}{\rho_e u_e^2} = \frac{f''_w}{\sqrt{2}}\left(\frac{\rho_w\mu_w}{\rho_e\mu_e}\right)^{0.12}\left(\frac{\rho_e u_e \bar{x}}{\mu_e}\right)^{-1/2} \tag{23}$$

From Fig. 6, f''_w can be determined for values of $\bar{\beta}$ and g_w.

VI. APPLICATION OF SIMILARITY SOLUTIONS

In predicting heat transfer from laminary boundary layers to arbitrary surfaces, free-stream and boundary conditions usually are such that requirements Eq. (10) for similarity solutions are not satisfied. Of these requirements only a constant wall enthalpy can be nearly realized in practice by wall cooling. One must then resort to solutions of the integral form of the boundary layer equations, finite difference numerical techniques or other methods (e.g., Hayes and Probstein, Ref. 14). Alternatively, the approximation of local similarity can be employed and known similarity solutions utilized. In the local similarity method the boundary layer profiles at a position along the surface are assumed identical to the similar profiles which would exist for the local free-stream condition. To justify this method the free-stream conditions should vary slowly along the surface, or, if these variations are not small, the dimensionless enthalpy gradient at the wall, to which the wall heat flux is related, should be rather insensitive to the free-stream velocity gradient parameter $\bar{\beta}$.

The criterion that the variation of g'_w along the surface be small compared to g'_w itself is usually satisfied for flows over blunt-nosed bodies since values of $\bar{\beta}$ are not large. Kemp et al. (Ref. 7), by considering the nonsimilar terms that would appear on the right side of Eq. (5) and (6) if the distributions f' and g also depend on ξ, express this as $2\xi\, d(g'_w/Pr)/d\xi << g'_w/Pr$. Lees (Ref. 6), noting this small variation in g'_w, selected an average value of $g'_w/(1 - g_w) = 0.50$ for which reasonably good agreement was found by Kemp et al. (Ref. 7) by comparison to their heat transfer measurements on the front side of blunt-nosed bodies in supersonic flow.

For internal flows, however, values of $\bar{\beta}$ can be quite large. To indicate the magnitude and variation of β for supersonic nozzle flow, values are shown in Fig. 7 for circular-arc-throat conical nozzles. It is seen that values of $\bar{\beta}$ vary greatly through the nozzle and reach values as large as 20 near the throat. If the nozzle wall is highly cooled, $g_w \cong 0$, then the variation of g'_w from Fig. 4 over the range of $0 \leq \bar{\beta} \leq 20$ is less than 15%. Details of the calculation of $\bar{\beta}$ for one-dimensional isentropic flow and its dependence on nozzle configuration are given in Appendix B. Though deviations from one-dimensional flow, especially in the throat region, have been found experimentally in circular-arc-throat conical nozzles (Ref. 15), the influence on g'_w would be small because of the weak dependence on $\bar{\beta}$ when $\bar{\beta}$ is large, as can be seen in Fig. 4.

The previous example illustrates a flow in which $\bar{\beta}$ is large; in fact, the analysis of this report was motivated by interest in predicting heat transfer from a laminar boundary layer to a cooled supersonic nozzle wall.

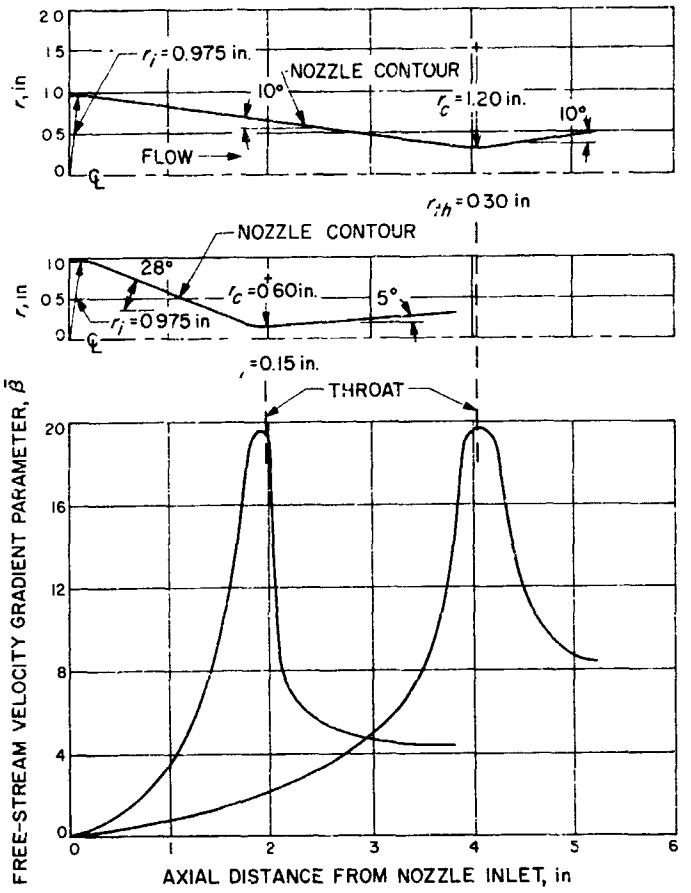

Fig. 7. Variation of free-stream velocity gradient parameter $\bar{\beta}$ with axial distance for two nozzles

Though similarity requirements are generally not satisfied for nozzle flow, the less than 15% variation of g'_w in particular for the nozzles shown in Fig. 7 may still not be large enough to invalidate the use of similarity solutions on a local basis to predict the wall heat flux [for special nozzle shapes the solutions of Coles (Ref. 8) and Lam (Ref. 16) are available]. An appraisal of the approximate method, which involves a minimum amount of calculation time, rests in comparison with experimental results.

In comparison with experimental results an important consideration in the application of the similarity solutions is where the prediction is started. Some insight on this, as well as supporting the direct application of the similarity solutions, is provided by a solution of the energy equation in the von Mises form, simplified by the slug flow approximation, i.e., the local velocity is taken at its free-stream value. For $Pr = 1$ and $C = 1$ the energy Eq. (3) is

$$\frac{\partial g}{\partial \xi} = \frac{\partial^2 g}{\partial \psi^2} \tag{24}$$

The new variable ξ is identical to that in the combined Levy-Mangler transformation Eq. (4) and ψ is the stream function. From the solution

$$g = 1 - (1 - g_w)\, erfc\left(\frac{\psi}{2\sqrt{\xi}}\right) \tag{25}$$

the heat flux to the wall, assumed isothermal downstream of where cooling begins ($\xi = 0$), is identical to that from the similarity solution of Eq. (8) except that $\sqrt{2/\pi} = 0.7979$ replaces $g'_w/(1 - g_w)$. The constant 0.7979 is the penalty for neglecting the actual velocity distribution and how it varies mainly with free-stream velocity gradient and wall cooling. As noted, ξ is related to the cooled length, i.e., $\xi = 0$ at the location $x = 0$ where cooling begins.

It is well known for low-speed, constant property flow over a flat plate that the heat flux predicted by assuming slug flow exceeds the actual value by the ratio $(1/\sqrt{\pi})/0.332 = 1.70$ for $Pr = 1$ (e.g., see Eckert and Drake, Ref. 17, p. 299). With flow acceleration the velocity distribution becomes steeper near the wall (e.g., see the Hartree wedge flows, Ref. 10) so that the slug flow approximation becomes more realistic, as indicated by the value 0.7979 compared to those values of $g'_w/(1 - g_w)$ shown in Fig. 4 for large values of $\bar{\beta}$. In fact, Coles (Ref. 8) in treating the case where $\bar{\beta} \to \infty$ found that the ratio of thermal to velocity layer thickness is of order $\sqrt{\bar{\beta}}$. For such a situation the slug flow approximation becomes very good, and this undoubtedly leads to the general correspondence between it and Coles' solution as $\bar{\beta} \to \infty$; for $g_w = 1.0$, the solutions are identical. Since wall cooling reduces the steepness of the velocity distribution near the wall, the slug flow approximation becomes worse; this trend is also observable in Fig. 4.

Unlike g'_w in the heat flux expression, the dimensionless velocity gradient at the wall f''_w, to which the wall shear stress is related, is strongly dependent on $\bar{\beta}$. Thus, the local similarity method does not appear to be applicable in predicting the wall shear stress unless, for the particular range of $\bar{\beta}$ of interest, the predicted variation of f''_w is small.

VII. CONCLUSIONS

Laminar boundary layer heat transfer and wall shear stress predictions from similarity solutions have been obtained in an approximate way over a large range of values of the free-stream velocity gradient parameter $\bar{\beta}$ and wall cooling. The solutions indicate that the application of the similarity solutions on a local basis to predict heat transfer to arbitrary surfaces, as has been demonstrated by Lees for lower $\bar{\beta}$ flows, may be a reasonable approximation over a larger range of $\bar{\beta}$ for accelerated flows, like those attainable in supersonic nozzles. In this regard comparisons to experimental results are needed. The local similarity method, however, does not appear to be applicable in predicting the wall shear stress, except for flows where the variation of $\bar{\beta}$ is small.

NOMENCLATURE

C dimensionless function, $\rho\mu/\rho_e\mu_e$

c_f friction coefficient, $c_f/2 = \tau/\rho_e u_e^2$

c_p specific heat at constant pressure

f' dimensionless velocity, u/u_e
f''_w gradient at wall

g dimensionless total enthalpy, H_t/H_{to}
g'_w gradient at wall

H static enthalpy

H_t stagnation enthalpy, $H + u^2/2$

k thermal conductivity

M Mach number

$\dot{m}$ mass flow rate

p static pressure

Pr Prandtl number

q heat flux to wall

r body or channel radius

r_c nozzle throat radius of curvature

r_{th} nozzle throat radius

R gas constant or recovery factor

St Stanton number

T static temperature

T_t stagnation temperature

u, v components of velocity parallel and normal to wall

x distance along wall

$\bar{x}$ length defined in Eq. (19)

y distance normal to wall

β free-stream velocity gradient parameter, $(2\xi/u_e)(du_e/d\xi)$

$\bar{\beta}$ free-stream velocity gradient parameter, $\beta(T_{to}/T_e)$

γ specific heat ratio

η dimensionless coordinate normal to wall, Eq. (4)

μ viscosity

ξ coordinate along wall, Eq. (4)

ρ density

τ wall shear stress

ψ stream function

ω exponent of viscosity–temperature relation

Subscripts

$_{aw}$ adiabatic wall condition

$_e$ conditions at free-stream edge of boundary layer

$_o$ reservoir condition

$_w$ wall condition

APPENDIX A

SOLUTIONS FOR $\bar{\beta} \to \infty$

In the limiting case as $\bar{\beta} \to \infty$, Coles' (Ref. 8) wall heat transfer and shear stress parameters are specified in terms of his zero-order functions g_0, h_0 and f_0

$$-\frac{I'(0)}{H_w} = -\frac{1}{\sqrt{\bar{\beta}}}\frac{h_0'(0)}{H_w}$$
$$G''(0) = g_0''(0) + \frac{1}{\sqrt{\bar{\beta}}} f_0''(0) \tag{A-1}$$

In our nomenclature these parameters are

$$-\frac{I'(0)}{H_w} = \frac{1}{\sqrt{\bar{\beta}}}\frac{g_w'}{1-g_w}$$

and

$$G''(0) = \frac{f_w''}{\sqrt{\bar{\beta}}};$$

also $H_w = g_w - 1$.

An exact solution for g_0 was obtained by Coles from which

$$g_0''(0) = \sqrt{\frac{4}{3}}\, g_w^{3/4} \tag{A-2}$$

The remaining two functions h_0 and f_0 satisfy the differential equations

$$h_0 + 1 - (f_0')^2 = 0 \quad \text{or} \quad f_0' = \sqrt{h_0 + 1} \tag{A-3}$$

$$h_0'' + f_0 h_0' = 0 \tag{A-4}$$

and boundary conditions

$$f_0(0) = 0,\ f_0'(0) = g_w^{1/2} \quad \text{or} \quad h_0(0) = g_w - 1$$
$$f_0'(\infty) = 1,\ h_0(\infty) = 0 \tag{A-5}$$

Shown in Table A-1 are values $g_w'/(1 - g_w)$ and $f_0''(0)$ obtained from Coles' approximate solution of Eq. (A-3) and (A-4) with boundary conditions Eq. (A-5) (note that $h_0'(0) = g_w'$). Also shown in Table A-1 are exact solutions of these equations obtained by Beckwith and Cohen (Ref. 9) for $g_w = 0$, ½ and 1 and, by us for intermediate values of $g_w = 0.2$, 0.6, and 0.8, as well as for $g_w = 0$ and ½. An exact solution is possible for $g_w = 1.0$ for which

$$\frac{g_w'}{1-g_w} = \sqrt{\frac{2}{\pi}} = 0.7979$$

Our calculations were made on an IBM 7094 computer by numerical integration with a variant of the Gill Modification (Ref. 18) of fourth-order Runge-Kutta used; the step size was $\Delta\eta = 0.0005$. By comparison in Table A-1, Coles' approximate solution yields values of $g_w'/(1 - g_w)$ and $f_0''(0)$ which are larger than the exact values as g_w decreases.

Table A-1. Results as $\bar{\beta} \to \infty$

g_w	Coles' approximate solution (Ref. 8)	Exact solution	Beckwith and Cohen (Ref. 9)	Coles' approximate solution (Ref. 8)	Exact solution
	$g_w'/(1 - g_w)$			$f_0''(0)$	
0	0.652	0.5901	0.58928	∞	∞
0.2	0.695	0.6590	—	0.624	0.5894
0.5	0.741	0.7234	0.72302	0.262	0.2558
0.6	0.754	0.7408	—	0.195	0.1913
0.8	0.777	0.7717	—	0.0870	0.0863
1.0	0.7979	0.7979	0.7979	0	0

APPENDIX B

CALCULATION OF $\bar{\beta}$ FOR AXISYMMETRIC NOZZLE FLOW

For one-dimensional isentropic flow the expression for $\bar{\beta}$ from Eq. (15) is

$$\bar{\beta} = \left(\frac{2}{u_e}\frac{du_e}{dx}\right)\frac{\xi}{\frac{d\xi}{dx}}\frac{T_{to}}{T_e} = -\frac{\frac{4}{r}\frac{dr}{dx}}{(1-M_e^2)}\frac{\int_0^x \mu_e dx}{\mu_e}\frac{T_{to}}{T_e} \tag{B-1}$$

The first factor in Eq. (B-1) is the familiar relation obtained from the combined continuity and momentum equations and the second factor was obtained from Eq. (4) for one-dimensional flow.

$$\xi = \frac{\dot{m}}{\pi}\int_0^x \mu_e dx \tag{B-2}$$

The calculations shown in Fig. 7 were initiated at the nozzle inlet (i.e., $\xi = 0$, $\bar{\beta} = 0$) with x the distance along the nozzle wall. The viscosity-temperature relation was taken as $\mu \alpha T^{0.64}$ and the specific heat ratio, $\gamma = 5/3$.

Since $\bar{\beta}$ is a maximum near the throat, the throat value $\bar{\beta}_{th}$ is of particular interest. The quantity

$$\frac{\frac{dr}{dx}}{1-M_e^2}$$

is indeterminate at the throat where $M_e = 1$, $dr/dx = 0$; however, by expanding r/r_{th} and M_e^2 in Taylor series about the throat, the following throat expression is obtained

$$\left[\frac{\frac{dr}{dx}}{1-M_e^2}\right]_{th} = -\sqrt{\frac{1}{2(\gamma+1)}}\sqrt{\frac{r_{th}}{r_c}} \tag{B-3}$$

where r_{th} is the throat radius and r_c the throat radius of curvature. By using

$$\frac{T_{to}}{(T_e)_{th}} = \frac{\gamma+1}{2}$$

and Eq. (B-3) the throat value is

$$\bar{\beta}_{th} = \sqrt{2(\gamma+1)}\,\frac{\frac{\bar{x}_{th}}{r_{th}}}{\sqrt{\frac{r_c}{r_{th}}}} \tag{B-4}$$

where $\bar{x}_{th}$ is an effective length to the nozzle throat, and is given by the second factor in Eq. (B-1). From Eq. (B-4), $\bar{\beta}_{th}$ is seen to increase with small r_c/r_{th} and large $\bar{x}_{th}/r_{th}$. Thus values of $\bar{\beta}_{th}$ shown in Fig. 7 are nearly equal, since $\bar{x}_{th}/r_{th}$ is about the same for the two nozzles which have identical values of r_c/r_{th}.

REFERENCES

1. Cohen, C. B., and Reshotko, E., "Similar Solutions for the Compressible Laminar Boundary Layer with Heat Transfer and Pressure Gradient," NACA R-1293, 1956 (supersedes NACA TN-3325, 1955).
2. Levy, S., "Effect of Large Temperature Changes (including Viscous Heating) upon Laminar Boundary Layers with Variable Free-Stream Velocity," *Journal of Aeronautical Sciences*, vol. 21, No. 7, July 1954, pp. 459–474

REFERENCES (Cont'd)

3. Probstein, R. F., "Methods of Calculating the Equilibrium Laminar Heat Transfer Rate at Hypersonic Flight Speeds," *Jet Propulsion*, vol. 26, June 1956, pp. 497–499.

4. Cohen, C. B., and Reshotko, E., "The Compressible Laminar Boundary Layer with Heat Transfer and Arbitrary Pressure Gradient," NACA R-1294, 1956 (supersedes NACA TN-3326, 1955).

5. Reshotko, E., "Simplified Method for Estimating Compressible Laminar Heat Transfer with Pressure Gradient," NACA TN-3888, 1956.

6. Lees, L., "Laminar Heat Transfer over Blunt-Nosed Bodies at Hypersonic Flight Speeds," *Jet Propulsion*, vol. 26, April 1956, pp. 259–269.

7. Kemp, N. H., Rose, P. H., and Detra, R. W., "Laminar Heat Transfer Around Blunt Bodies in Dissociated Air," *Journal of the Aero-Space Sciences*, vol. 26, July 1959, pp. 421–430.

8. Coles, D., "The Laminar Boundary Layer Near a Sonic Throat," *Heat Transfer and Fluid Mechanics Institute*, 1957, pp. 119-137.

9. Beckwith, I. E., and Cohen, N. B., "Application of Similar Solutions to Calculation of Laminar Heat Transfer on Bodies with Yaw and Large Pressure Gradient in High-Speed Flow," NASA TN-D-625, Jan. 1961.

10. Schlichting, H., *Boundary Layer Theory*, McGraw-Hill Book Co., Inc., New York, Fourth Edition, 1960.

11. Bade, W. L., "Stagnation-Point Heat Transfer in a High-Temperature Inert Gas," *Physics of Fluids*, vol. 5, No. 2, Feb. 1962, pp. 150–154.

12. Fay, J. A., and Riddell, F. R., "Theory of Stagnation Point Heat Transfer in Dissociated Air," *Journal of the Aeronautical Sciences*, vol. 25, No. 2, Feb. 1958, pp. 73–85.

13. Gross, J. F., and Dewey, C. F., *Similar Solutions of the Laminar Boundary Layer Equations with Variable Fluid Properties*, Memorandum RM-3792-PR, The Rand Corporation, Santa Monica, California, Aug. 1963.

14. Hayes, W. F., and Probstein, R. F., *Hypersonic Flow Theory*, Academic Press, New York and London, 1959.

15. Back, L. H., Massier, P. F., Gier, H. L., *Comparison of Experimental with Predicted Wall Static-Pressure Distributions in Conical Supersonic Nozzles*, Technical Report No. 32-654, Jet Propulsion Laboratory, Pasadena, California, October 15, 1964.

16. Lam, S. H., "Interactions of Heat Transfer and Hypersonic Boundary Layers under Highly Favorable Pressure Gradients," *Heat Transfer and Fluid Mechanics Institute*, 1963, pp. 44–57.

17. Eckert, E. R. G., and Drake, R. M., *Heat and Mass Transfer*, McGraw-Hill Book Co., Inc., New York, Second Edition 1959, p. 299.

18. Ralston, A., and Wilf, H. S., *Mathematical Methods for Digital Computers*, John Wiley and Sons, Inc., New York, 1960, p. 110.